Widespread Distribution of Soluble Di-Iron Monooxygenase (SDIMO) Genes in Arctic Groundwater Impacted by 1,4-Dioxane

Mengyan Li,[†] Jacques Mathieu,[†] Yu Yang,[†] Stephanie Fiorenza,[‡] Ye Deng,[§] Zhili He,[§] Jizhong Zhou,[§,∥,⊥] and Pedro J. J. Alvarez*,[†]

[†]Department of Civil and Environmental Engineering, Rice University, Houston, Texas, United States

[‡]Remediation Engineering and Technology, BP America, Houston, Texas, United States

[§]Institute for Environmental Genomics, Department of Microbiology and Plant Biology, University of Oklahoma, Norman, Oklahoma, United States

[∥]State Key Joint Laboratory of Environment Simulation and Pollution Control, School of Environment, Tsinghua University, Beijing, China

[⊥]Earth Sciences Division, Lawrence Berkeley National Laboratory, Berkeley, California, United States

S *Supporting Information*

ABSTRACT: Soluble di-iron monooxygenases (SDIMOs), especially group-5 SDIMOs (i.e., tetrahydrofuran and propane monooxygenases), are of significant interest due to their potential role in the initiation of 1,4-dioxane (dioxane) degradation. Functional gene array (i.e., GeoChip) analysis of Arctic groundwater exposed to dioxane since 1980s revealed that various dioxane-degrading SDIMO genes were widespread, and PCR-DGGE analysis showed that group-5 SDIMOs were present in every tested sample, including background groundwater with no known dioxane exposure history. A group-5 *thmA*-like gene was enriched (2.4-fold over background, $p < 0.05$) in source-zone samples with higher dioxane concentrations, suggesting selective pressure by dioxane. Microcosm assays with ^{14}C-labeled dioxane showed that the highest mineralization capacity (6.4 $\pm$ 0.1% $^{14}CO_2$ recovery during 15 days, representing over 60% of the amount degraded) corresponded to the source area, which was presumably more acclimated and contained a higher abundance of SDIMO genes. Dioxane mineralization ceased after 7 days and was resumed by adding acetate (0.24 mM) as an auxiliary substrate to replenish NADH, a key coenzyme for the functioning of monooxygenases. Acetylene inactivation tests further corroborated the vital role of monooxygenases in dioxane degradation. This is the first report of the prevalence of oxygenase genes that are likely involved in dioxane degradation and suggests their usefulness as biomarkers of dioxane natural attenuation.
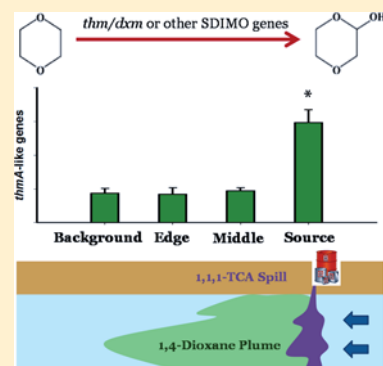
■ INTRODUCTION

1,4-Dioxane (dioxane) is a cyclic ether that is widely used as a stabilizer for chlorinated solvents (mainly 1,1,1-trichloroethane [1,1,1-TCA]).[1] Dioxane is a suspected carcinogen[2] and is subject to a stringent drinking water advisory level of 0.35 μg/L, corresponding to a 10^{-6} increased lifetime cancer risk.[3] Clean-up of dioxane-contaminated sites is a difficult task because of its recalcitrance to biodegradation and physicochemical properties that preclude effective removal by volatilization or adsorption. Furthermore, dioxane tends to migrate further and impact larger areas than co-occurring chlorinated solvents.[1] This underscores the need for cost-effective alternatives to manage large and dilute dioxane plumes, which are not amenable to treatment by aggressive *in situ* remediation techniques, such as *in situ* chemical oxidation.[4]

Monitored natural attenuation (MNA), which relies primarily on intrinsic bioremediation, is often a cost-effective approach to manage trace levels of priority pollutants.[5] However, the burden of proof that MNA is an appropriate solution lies on the proponent, and MNA has not been widely used at dioxane-impacted sites because (1) the presence and expression of dioxane biodegradation capabilities are generally perceived to be rare in the environment, and (2) our ability to assess the feasibility and efficacy of intrinsic bioremediation is precluded by our very limited understanding of the diversity and spatial distribution of microorganisms that degrade dioxane. This underscores the importance to assess the distribution of dioxane degradation capabilities in different environments. Recent findings by our lab and others suggest that indigenous bacteria that can degrade dioxane might be more widespread than previously assumed, even in low productivity environments such as the Arctic tundra.[6−8] However, little is known about the *in situ* degradation pathways and associated genes/enzymes that could serve as biomarkers

for the forensic assessment of dioxane bioremediation and natural attenuation.

Soluble di-iron monooxygenases (SDIMOs) are multi-component bacterial enzymes that incorporate one oxygen atom from O_2 into various substrates such as chlorinated solvents, aromatic hydrocarbons, alkanes, and alkenes to initiate catabolism.[9] SDIMOs can be divided into five groups, based on component arrangement, substrate specificity, and sequence similarity.[9,10] Several SDIMOs (Table 1) are likely involved in

Table 1. Monooxygenases Implicated in Dioxane Degradation

gene name	monooxygenase (MO)	SDIMO group	representative bacterial strain	GenBank accession no.
thm	tetrahydrofuran MO	5	*Pseudonocardia* sp. K1	AJ296087
prm	propane MO	5	*Rhodococcus* sp. RR1	HM209445
tom	toluene-2-MO	1	*Burkholderia cepacia* G4	AF319657
tbu	toluene-3-MO	2	*Ralstonia picketii* PKO1	U04052
tmo	toluene-4-MO	2	*Pseudomonas mendocina* KR1	M65106
mmo	soluble methane MO	3	*Methylococcus capsulatus* Bath	M90050

the scission of the C−O bond for cyclic ethers such as dioxane and its structural analog, tetrahydrofuran (THF).[8,11−13] Moreover, a putative dioxane monooxygenase gene cluster (designated as *dxmADBC* in this paper) located in plasmid pPSED02 of the dioxane metabolizer *Pseudonocardia dioxanivorans* CB1190 has been identified.[11,14,15] This *dxm* cluster is highly homologous to the putative THF monooxygenase gene clusters for *Pseudonocardia* sp. K1, *Pseudonocardia* sp. ENV478, and *Rhodococcus* sp. YYL, based on the nucleotide sequence identity of each gene (e.g., > 97% for α subunit) as well as the arrangement of genetic components.[11,13,16] Moreover, among the eight multicomponent monooxygenases produced by CB1190, only this putative dioxane monooxygenase cluster showed significant up-regulation after amendment with dioxane.[17] Additional studies using Northern blot[11] and colorimetric naphthol assays[12] have implicated THF and dioxane monooxygenases as key enzymes that initiate dioxane catabolism through 2-hydroxylation.

Propane monooxygenases bear a close evolutionary relationship with THF/dioxane monooxygenases and are grouped in the same subdivision (group 5), although they do not share the same substrate range. However, dioxane cometabolism has been observed with bacteria containing propane monooxygenases. For instance, propane-grown *Rhodococcus ruber* ENV425 and toluene-grown *Rhodococcus* sp. RR1 can rapidly remove dioxane in aqueous solution with degradation rates of 0.01 mg/h/mg TSS and 0.38 mg/h/mg protein, respectively.[12,13] The degradation rate for the latter strain was twice as high as that of the metabolizer CB1190 (0.19 mg/h/mg protein).[12] A putative propane monooxygenase gene *prmA* was recently identified in RR1, whose nucleotide sequence and propane-inducible transcription are highly consistent with *prmA* from *Rhodococcus jostii* RHA1. Notably, an RHA1 *prmA* knockout mutant lacked the ability to metabolize propane.[18] Furthermore, a cultured propanotroph SL-D degraded at least 10 mg/L dioxane after the primary growth substrate (i.e., propane) was fully depleted.[19] Collectively, these reports implicate the potential

of propane monooxygenases to initiate dioxane cometabolism. Hence, it is likely that Group-5 SDIMOs (e.g., THF/dioxane and propane monooxygenases) play a crucial role in dioxane biodegradation. However, whether bacteria harboring such SDIMOs are enriched at dioxane-impacted sites is unknown.

This paper addresses the spatial distribution of SDIMO and other functional genes at a dioxane-impacted site on the north slope of Alaska. GeoChip[20−23] and PCR-DGGE were used to investigate the diversity and relative abundance of these functional genes along the dioxane plume and in background samples. Microcosm experiments with ¹⁴C-labeled dioxane were also conducted to discern dioxane mineralization patterns and determine whether samples with higher abundance of SDIMO genes exhibited a higher extent of dioxane mineralization. Accordingly, this paper is the first to document the presence of *thmA* and *prmA*-like genes in groundwater impacted by dioxane and thus contributes to the forensics of natural attenuation and bioremediation performance assessment for dioxane-impacted sites.

■ EXPERIMENTAL PROCEDURES

Site Description and Sample Collection. Groundwater samples were collected in August 2010 from a site on the north slope of Alaska. This site is an oil and gas industrial facility surrounded by Arctic tundra and was impacted by chlorinated solvents spills (especially 1,1,1-TCA), and thus the common stabilizer dioxane, since the 1980s. Natural attenuation studies in such remote cold region have received limited attention in the literature. To study the effect of dioxane on the indigenous microbial community, four monitoring wells (Figure 1) along the dioxane plume were sampled, including the source (MW201), the middle (MW11), and the leading-edge of the plume (MW33) as well as a background control from an area of no known prior exposure history (MW26).

Groundwater samples were collected using peristaltic pumps with sterile tubing. The wells were purged and sampled using low-flow techniques, and the temperature, pH, conductivity, and dissolved oxygen were monitored during the purging process. Samples were stored in 1-L sterile glass amber containers at 4 °C with minimum headspace. For each well, continuous water samples were collected in triplicate.

Chemical Characterization. Samples were analyzed by Pace Analytical Services, Inc. (Minneapolis, MN) for Volatile Organic Compounds by EPA method 8260, Semi-Volatile Organic Compounds by EPA method 8270, Polycyclic Aromatic Hydrocarbons by EPA method 8270 SIM, Diesel-Range Organics by Alaska method 102, Alkalinity by E310.1, and Methane, Ethane, and Ethane by RSK175. Dioxane concentrations for all replicate samples (Table 2) were also measured by a novel frozen microextraction method,[24] followed by quantification with GC/MS in the Selective Ion Monitoring (SIM) mode.

DNA Extraction. Approximately 500 mL of each sample replicate was filtered through a 0.22-μm cellulose membrane (Millipore, Billerica, MA) to collect the biomass. Microbial genomic DNA isolation was performed by combining Tris buffer extraction, liquid nitrogen freeze grinding, and sodium dodecyl sulfate (SDS) cell lysis as previously described.[25] DNA purity was determined by UV spectroscopy using an ND-1000 Spectrophotometer (NanoDrop, Wilmington, DE). To minimize bias for microarray hybridization, a high absorbance ratio at 260 nm/230 nm (>1.7) and 260 nm/280 nm (>1.8) was required. Quant-iT PicoGreen dsDNA Assay kit (Invitrogen,
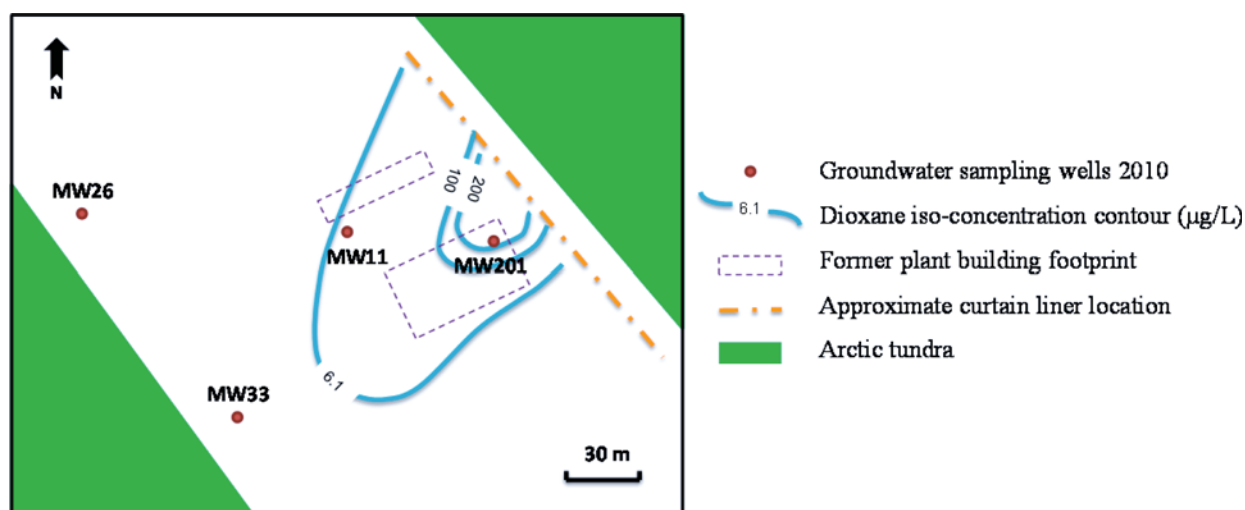
Figure 1. Four groundwater locations sampled in 2010 and dioxane iso-concentration contour based on 2008 analysis data.

Table 2. Dioxane and 1,1,1-TCA Concentrations (μg/L) in the Four Groundwater Samples

monitoring well	sampling location description	dioxane		1,1,1-TCA
		P&T[a]	FME[b]	
Source (MW 201)	plume center with maximum dioxane concentration	590	560.5 ± 11.9	3490
Middle (MW 11)	down-gradient of the plume center with dioxane concentration greater than 6.1 μg/L (i.e., the Tier 1 groundwater screening level at Alaska)	18.3	10.4 ± 0.8	ND (<0.090)
Edge (MW 33)	leading edge of the dioxane with trace level of dioxane (<6.1 μg/L)	3	2.5 ± 0.3	0.3
Background (MW 26)	away from the dioxane plume without contamination	ND[c] (<3)	ND (<1.6)	ND (<0.090)

[a]P&T = purge and trap. Dioxane concentrations in this column were analyzed in a commercial lab using EPA method 8260 followed by GC/MS.
[b]FME = frozen microextraction. Dioxane concentrations in this column were measured in our lab using frozen microextraction followed by GC/MS.
[c]ND = not detected. The value in parentheses is the method detection limit for this measurement.

Carlsbad, CA) was then used to selectively quantify the double-stranded DNA before further treatment according to the manufacturer's protocol.

GeoChip 4.0 Hybridization and Data Analysis. Geo-Chip 4.0, a high-throughput microarray-based technology, was used to characterize the diversity of microbial functional genes related to organic remediation present in the samples. This functional gene array can target 410 gene categories covering essential biogeochemical cycles, energy processing, organic contaminant degradation, and stress responses.[6,20,23,26]

A total amount of 1.5 μg of the purified genomic DNA for each replicate was directly labeled with fluorescent dye Cy-3. After preheating, aliquots of labeled DNA mixtures were loaded onto each array of a single GeoChip 4.0 slide. After hybridization with mixing on a Hybridization Station (MAUI, BioMicro Systems, Salt Lake City, UT) at 42 °C plus 40% formamide for 16 h, the microarray slide was washed and scanned by MS 200 Microarray Scanner (NimbleGen, Madison, WI) at a laser power of 100%. The procedures for GeoChip hybridization, scanning, and data processing were introduced in detail in the Supporting Information as previously described.[6,20,27] The detection limit for this functional gene array is 50 to 100 ng dsDNA when more than 50% expected oligonucleotide probes are detected.[28]

To eliminate singletons among replicates, a gene was retrieved only when a positive hybridization signal was obtained for more than one replicate. Then, the fluorescence signal of each gene in a groundwater sample was calculated as the average of its replicates. Hierarchical clustering was performed in Cluster 3.0 using the pairwise complete-linkage hierarchical clustering algorithm, and heatmaps were visualized using TreeView with centered correlation mode for both arrays and genes.[29] Whether differences in absolute fluorescent signal intensities between samples were significant was assessed statistically using ANOVA at the 95% confidence level. Canonical correlation analysis (CCA)[30] was conducted to examine the influence of various environmental factors on the abundance of functional gene structures. Mantel test[31,32] was used to assess the relationship between microarray data and different contaminants in the groundwater.

PCR-DGGE. Denaturing Gradient Gel Electrophoresis (DGGE) was used to assess the diversity of SDIMOs in the groundwater samples. Two pairs of degenerate primers were designed by Coleman et al. based on the conservative regions of the α subunit of SDIMOs.[33] Due to a low abundance of SDIMO genes in the groundwater samples, a nested PCR strategy was used to produce sufficient amplicons as detailed in the Supporting Information. In this case, only SDIMOs in group 4 (alkene degrading genes) and 5 (cyclic ether degrading genes) were recovered by the secondary PCR.[34]

Resulting fragments of SDIMOs were then mixed with equal volume of 2 × loading buffer and loaded onto an 8% polyacrylamide gel with a denaturing gradient from 30% to 80% (where 100% denaturant corresponds to 7 M urea and 40% formamide).[35] Gradient Maker (GM-100) (CBS Scientific, Del Mar, CA) helped to ensure a reproducible uniform
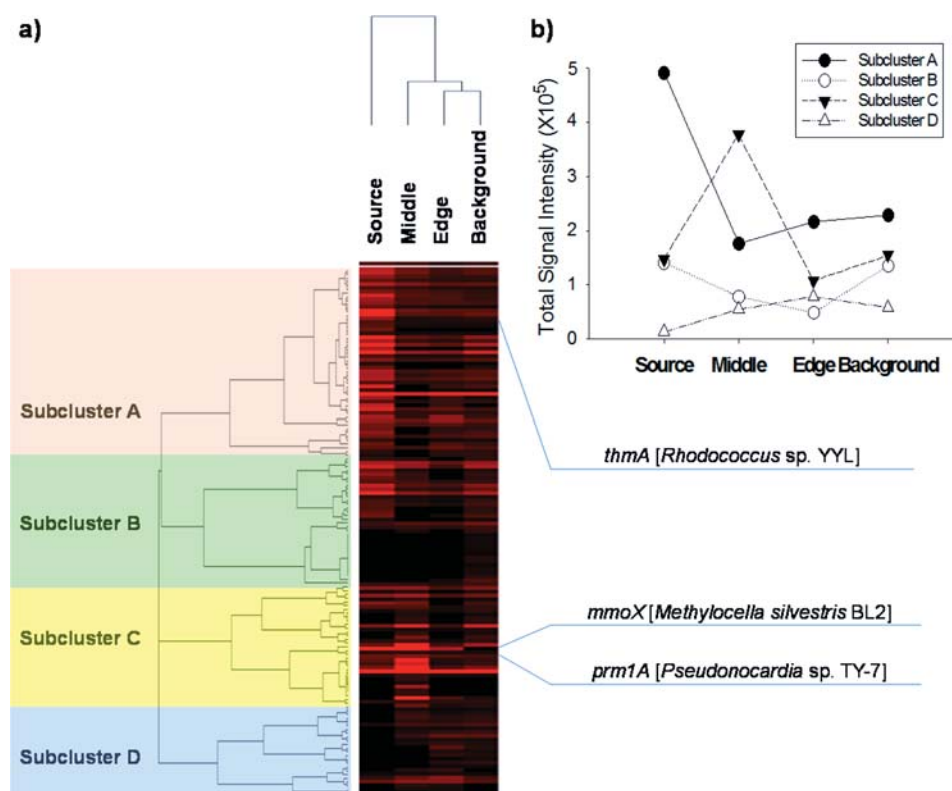
Figure 2. Hierarchical cluster analysis of SDIMO genes detected by GeoChip 4.0. Red indicates positive averaged signal intensities of the replicates at each sampling location, and black indicates intensities below background. Representative organisms for selected genes are depicted on the right of the heat map. Genbank ID, Gene name, and fluorescent intensities of detected SDIMOs are given in Table S1 in the SI. SDIMO genes were divided into four subclusters based on correlations of their relative abundance distribution patterns among different sampling locations (a). The total signal intensities in each subcluster are provided for each sampling location (b). Subcluster A genes, which included *thmA*, were enriched at the source, while Subcluster C genes were dominate in the middle of the plume.

denaturing gradient for gel casting. Electrophoresis was performed at 60 °C for 16 h at a constant voltage of 100 V using DCode universal mutation detection system (BioRad, Hercules, CA). Then the gel was stained, and visualized bands were excised and sequenced (Supporting Information). After combining the sequence reading from either side, the trimmed sequences were translated into amino acid sequences and then clustered using Cluster X 2.1.[36] The phylogenetic tree based on translated amino acid sequences was then visualized by MEGA 5.1.[37]

Mineralization Assays. Mineralization of ^{14}C-labeled dioxane was assessed by capturing ^{14}CO$_2$ released by microbial respiration in NaOH traps, as previously described.[38] Microcosms were prepared with 50 mL of groundwater sample and 50 mL of Ammonia Mineral Salt (AMS) media and amended with 25 μL of uniformly ^{14}C-labeled 1,4-dioxane (10-μCi/mL, > 99% purity, ChemDepo, Inc., CA). ^{14}CO$_2$ was trapped in a 10-mL glass vial containing 5 mL of 1 M NaOH adhered to the bottom of an amber bottle. ^{14}CO$_2$ and the remaining radioactivity in the liquid media were monitored by liquid scintillation counting (LS 6500, Beckman scintillation counter, Brea, CA). Six replicates were prepared for each treatment.

To assess the potential accumulation of ^{14}C-labeled dioxane metabolites, filtered water samples were analyzed by high-performance liquid chromatography (Shimadzu, Kyoto, Japan) coupled with radiochromatographic detector (IN/US Systems, Inc., Tampa, FL) (HPLC-RC). Separation was achieved with a Delta Pak C18 column (150 mm × 3.9 mm i.d., 300 Å, Waters, Milford, MA) at a constant flow rate of 1 mL/min with a

mobile phase of 50% methanol and 50% DI water. The detection limit for the HPLC-RC was 0.4 nCi/mL.

■ **RESULTS AND DISCUSSION**

Widespread Distribution of SDIMO Genes in Group 5. Microarray hybridization results revealed the presence of all five groups of SDIMO genes at the four sample sites, including a putative THF monooxygenase gene (*thmA*) from a known THF degrader (*Rhodococcus* sp. YYL),[16] at all four samples (Figure 2). This gene encodes the α subunit of a hydroxylase protein and possesses 99% nucleotide sequence identity with the *dxmA* gene from CB1190. Surprisingly, this putative dioxane-degrading gene was present in samples with no known history of dioxane contamination. The presence of *thmA* was corroborated by PCR-DGGE analysis. The prevailing Band F (Figure 3) at the site shares 98% amino acid sequence identity with the large hydroxylase from *P. dioxanivorans* CB1190 and 97% amino acid sequence identity with those from YYL, K1, and ENV478 (Figure 4).[11,13,16] Moreover, another *thmA*-like gene (Band I) was found in samples from the middle of the plume (MW11). This suggests that bacteria (probably Actinomycetales) harboring THF/dioxane monooxygenases may be widespread in the Arctic groundwater. This is the first study to document the presence of THF/dioxane monooxygenase genes in groundwater samples.

Six predicted propane monooxygenase genes were detected by GeoChip, including *prm1A* encoding one of the two propane monooxygenase hydroxylase α subunits produced by *Pseudonocardia* sp. TY-7. Notably, the chromosome of CB1190
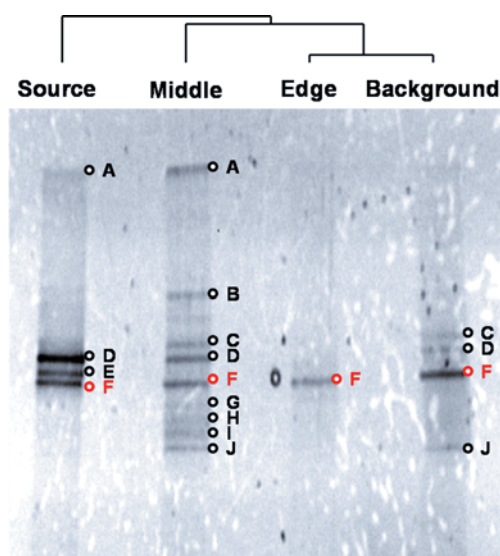
Figure 3. DGGE gel photograph showing the heterogeneous presence of SDIMOs by nested PCR (NVC58 and NVC65 as the primers for the first PCR set and then NVC57 + GC clamps and NVC66 as the primers for the second PCR set). Band F (highlighted in red) was found at all four sampling locations and corresponds to a *thmA*-like gene (Figure 4). Optical absorbance peaks of each band are given in Table S2 in the SI.

contains a putative propane monooxygenase, which shares high similarity to the *prm1ABCD* gene cluster of TY-7. The identity between the amino acid sequences of these two *prmA* genes is 85%. The coexistence of both *thm/dxm* and *prm* genes is not unique for CB1190. Other dioxane degraders from the *Pseudonocardiaceae* family, such as strain K1, also possess *prm* genes in their genome (data not shown). Moreover, propane supports the growth of *thm*-harboring ENV478, which can then

degrade dioxane, MTBE, and other ethers.[13] Thus, the co-occurrence of both genes detected at all sampling locations might imply the presence of bacteria, especially Actinomycetales, serving a similar function as those dioxane degraders.

In accordance with the microarray results, several putative propane monooxygenases were identified by PCR-DGGE (Figure 4). Except for Bands F and I, sequences of all other bands were annotated as *prmA*-like genes. The amino acid sequences recovered from Bands G, H, and J showed very high similarity (>87%) to the large hydroxylase subunit *prm1A* of the propane monooxygenase from *Pseudonocardia* sp. TY-7. All three bands were found in the sample from the middle of the plume, which corroborates their high signal intensities of the *prm1A* gene seen by microarray (Figure 2a). However, no such bands were found in the source and leading-edge samples. Interestingly, sequence fragments recovered from Bands C, D, and E were closely related to the other large hydroxylase subunit gene harbored by strain TY-7, *prm2A*, with sequence identities ranging from 81 to 88%. Both *prm1A* and *prm2A* are highly up-regulated when fed with propane as determined by Northern blot analysis.[39] Only Band B was annotated as a Proteobacteria *prm* gene, and it is probable that all other *prm* genes are from indigenous Actinomycetales at the site. For most of the bands, the corresponding sequences are similar to the *prmA*-like genes previously discovered in environmental soil and sediment samples.[33]

Our discovery of previously unreported *prmA*-like genes, while not surprising, reveals a greater diversity of propane monooxygenases in the environment than expected and suggests that propane may be a candidate primary substrate to biostimulate dioxane bioremediation. Propane has been used as a substrate for TCE cometabolism, with performance exceeding that of methane or butane.[40] Moreover, propanotrophs might outcompete methanotrophs in the presence of background copper, which inhibits soluble methane mono-
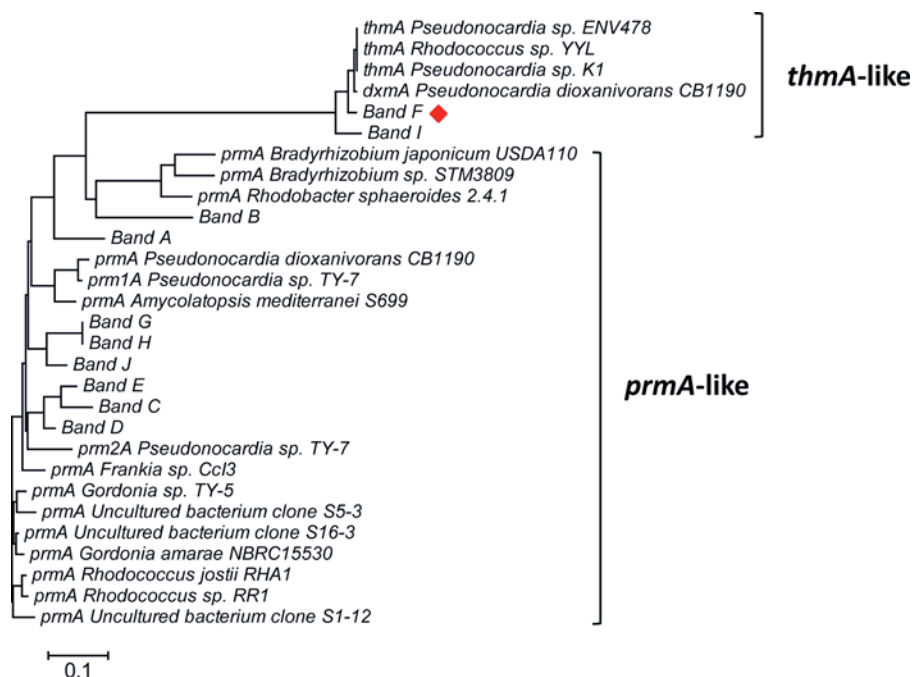
Figure 4. Neighbor-joining tree showing the genetic relationships between the translated SDIMO amino acid sequences recovered from each DGGE band and some annotated and predicted *prmA* and *thmA* genes from cultured or uncultured bacteria in GenBank. The prevailing Band F was highlighted with a red diamond.

oxygenase expression.[41] Successful removal of dioxane in microcosms amended with propanotrophs has been achieved when the initial concentration of dioxane was as high as 10 mg/L.[42]

Enrichment of the *thmA*-like Genes near the Source Zone. ANOVA analysis (Figure 5) indicated a 2.4-fold
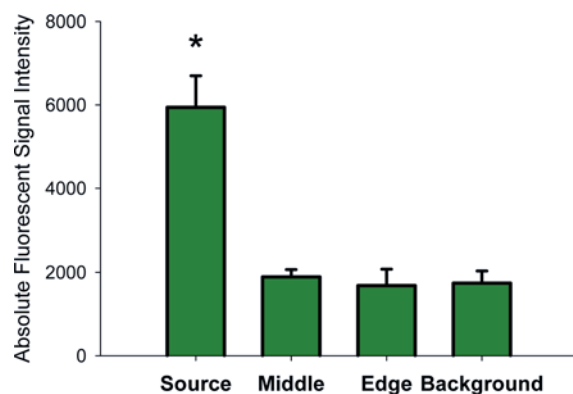
Figure 5. Absolute fluorescent signal intensities of the *thmA* gene in Arctic groundwater samples detected by GeoChip 4.0. The asterisk (*) indicates significant enrichment as determined by ANOVA.

enrichment for the *thmA* gene detected by GeoChip 4.0 ($p < 0.05$) in source-zone samples that were presumably more acclimated, despite dioxane representing a small fraction of the total dissolved organic carbon at this site (Table S3). Dioxane concentrations in the source zone were significantly ($p < 0.05$) higher than those at all other locations (Table 2), suggesting selective pressure by dioxane. Note that we have found microarray results to be conservative, providing very few false positives and generally underestimating the actual level of enrichment.[43]

The presence of *thm*-like genes was further verified using PCR-DGGE (Figure 3). Band F, encoding a *thm*-like gene that is 97% identical to the *thmA* gene detected by microarray, exhibited higher absorbance for the source zone samples than other locations (Table S2), corroborating the enrichment of the *thm* near the source zone. The prevalence of *thm*-like genes may reflect not only proliferation associated with dioxane metabolism but also the fact that *thm* genes tend to be harbored in plasmids,[11,14] which may facilitate horizontal gene transfer under selective pressure.

Spatial Distribution of Other SDIMO Genes. In addition to the SDIMO genes from group 5 (THF and propane monooxygenases), the remaining groups of SDIMO genes were all detected by GeoChip array in the four sampling locations. These groups include phenol hydroxylases (*pheA*; Group 1), toluene monooxygenases (*tomA*; Group 1 and *tmoABE*; Group 2), methane and butane monooxygenases (*mmoX*; Group 3 and *BMO*; Group 3), and alkene monooxygenases (*Xamo*; Group 4). Based on the similarity of their abundance distribution patterns, four major SDIMO subclusters were formed (Figure 2a) using hierarchical clustering. The total signal intensities for each subcluster are shown in Figure 2b, which depicts the distribution trends.

In subcluster A, which includes the *thmA* gene mentioned above, genes in the source zone sample exhibited much higher signal intensities than in other locations. Additionally, a *tomA* gene from *Verminephrobacter eiseniae* EF01-2 was in this subcluster. This gene encodes the α subunit of a putative

toluene-2-monooxygenase, which oxidizes toluene and other aromatic compounds through the *ortho*-pathway.[46] A previous study demonstrated that the toluene-2-MO containing bacterial strain, *Burkholderia vietnamiensis* G4, was capable of co-oxidizing dioxane when induced by toluene.[12] Although it is uncertain whether many of the genes in subcluster A are involved in dioxane degradation, their significant enrichment as well as their high similarity to enzymes known to be active in cometabolism of dioxane suggest a potential role. Note that numerous substrates are present at this site, which could support the growth of many bacteria including some that harbor SDIMO genes, resulting in their fortuitous enrichment.[44−47]

In subcluster C, SDIMO genes in water samples from the middle of the plume showed greater signal intensities than from other locations, which may be caused by the high methane concentrations (19.4 mg/L) and high TOC in MW 11. The high methane concentration at this location might be due to the thawing gas hydrates in the permafrost beneath the subsurface groundwater in the summer time. In addition to the primary component methane, natural gas typically contains more than 5% of short-chain alkanes (i.e., ethane, propane, and iso-butane).[48] This may explain why the *prm1A* gene from TY-7 was in this subcluster. In addition, this subcluster contains three soluble methane monooxygenase genes (*mmoX*) and one butane monooxygenase gene (*bmoY*). In the absence of copper, soluble methane monooxygenases (not particulate ones) from methanotrophic bacteria can be specifically induced by methane and fortuitously degrade dioxane.[12] DGGE analysis (Figures 3 and 4) also reveals that most *prmA*-like genes were only abundant at this location. Subclusters B and D contain genes mostly detected in samples from the leading-edge of the plume and the background control.

Spatial Differences in Microbial Functional Structure. Microarray hybridization data suggest that the overall functional structure of the microbial community changed along the plume. First, the total number of detected genes decreased in samples with contaminants, ranging from 17,411 (source) to 22,980 (background) (Table S7). Second, both Shannon-Weaver index (H) and Simpson's diversity index (1/D) indicated a higher functional diversity for background samples. The Pielou evenness indexes (E) for different samples all approached 1, reflecting an even distribution of functional genes at each monitoring well location. Third, a high percentage of unique genes (12.6%) was found only in background samples (Table S8), while source-zone samples contained the fewest unique genes (3.4%). Despite the selective pressure exerted by contaminants at different points in the plume, all samples shared similar percentages of overlapping genes (62 to 67%), showing the 'relatedness' of the microbial communities at the site.

The influence of selected environmental variables on the spatial distribution of functional genes detected by GeoChip 4.0 was also investigated by CCA (Figure S3). The analysis grouped together background samples with samples from the leading-edge of the plume that had low dioxane concentrations (≤ 3 μg/L). Source and mid-plume samples were plotted in different quadrants. The biplot shows that the overall functional gene signal intensities in the source zone sample were positively correlated with the concentration of various contaminants, including dioxane, chlorinated solvents, and aromatic hydro-carbons. However, methane was the most influential factor

affecting the functional gene signal intensity patterns in the sample from the middle of the plume.

The four groundwater samples could be separated into three groups: (i) the well close to the source zone (MW201), which was highly impacted by dioxane, chlorinated solvents, and other aromatic hydrocarbons (Tables S3–S6); (ii) the well in the middle of the plume (MW11), where trace levels of contaminants were detected but with high concentrations of methane and organic matter; and (iii) two distant wells downgradient (MW33 and MW26), where impact by carbon sources was minimal. This distribution pattern is consistent with the hierarchical clustering pattern of 140 SDIMO genes detected among all samples (Figure 2a) as well as the DGGE bands (Figure 3) based on their optical absorbance and migration positions (Table S8).

Overall, converging lines of evidence suggest that selective pressure by various contaminants near the source zone have decreased the functional diversity of the microbial community by enriching microbes capable of assimilating the organic compounds. This trend is consistent with previous studies of polluted environments, such as oil-contaminated soils in China[22] and uranium-impacted groundwater in Oak Ridge, TN.[49,50]

Dioxane Mineralization Patterns. Microcosms prepared with source-zone samples exhibited the highest extent of mineralization (6.4 ± 0.1% over 2 weeks, representing about 60% of the dioxane degraded). Though relatively low, this extent of mineralization is commensurate with the relatively short incubation time during which dioxane concentrations decreased by about 10%, from 244.7 ± 4.1 μg/L to 217.8 ± 2.2 μg/L (Figure 6). It is highly unlikely that the recovered $^{14}CO_2$ was associated with radiolabeled impurities since the stock ^{14}C-dioxane was at least 99% pure, and no other radiolabeled peaks besides dioxane were detected by HPLC analysis with a radiochromatographic detector (Figure S5). Previous microcosm studies with samples collected from this site showed dioxane biodegradation at comparable rates (around 10 μg/L/week, versus, 13 μg/L/week in this study).[6] Studies with pure cultures have also reported similar extents of mineralization as a percentage of the amount degraded (e.g., over 60% by CB1190).[51]

No degradation lag (Figure 6) was observed for source zone microcosms, indicating a high degree of acclimation. All other microcosms experienced a lag for $^{14}CO_2$ production longer than one day (Figure S4). Significantly lower mineralization extent (5.1 ± 0.1%) was observed in microcosms prepared with groundwater collected from the middle of the plume. Similar mineralization patterns were observed in microcosms prepared with other samples (the leading-edge and unimpacted background) ($p > 0.05$). The extent of mineralization was as low as 3.6 ± 0.1% and 3.2 ± 0.3%, respectively. The recoveries for the total ^{14}C ranged from 87.1% to 99.6% during the 15-day incubation period.

Both dioxane depletion and mineralization ceased after one week of incubation. This cessation may be caused by either deficiency of enzymatic cofactors or inhibition by metabolites (e.g., 2-hydroxyethoxyacetic acid) that could accumulate.[13,51,52] However, HPLC-RC analysis indicated that no byproducts accumulated in the aqueous phase of the microcosms after 15-day incubation (Figure S5). Thus, at day 15, sodium acetate (0.24 mM) was added as an auxiliary substrate to provide the indigenous microbes with reducing equivalents (i.e., NADH) required for monooxygenase activity. The use of acetate
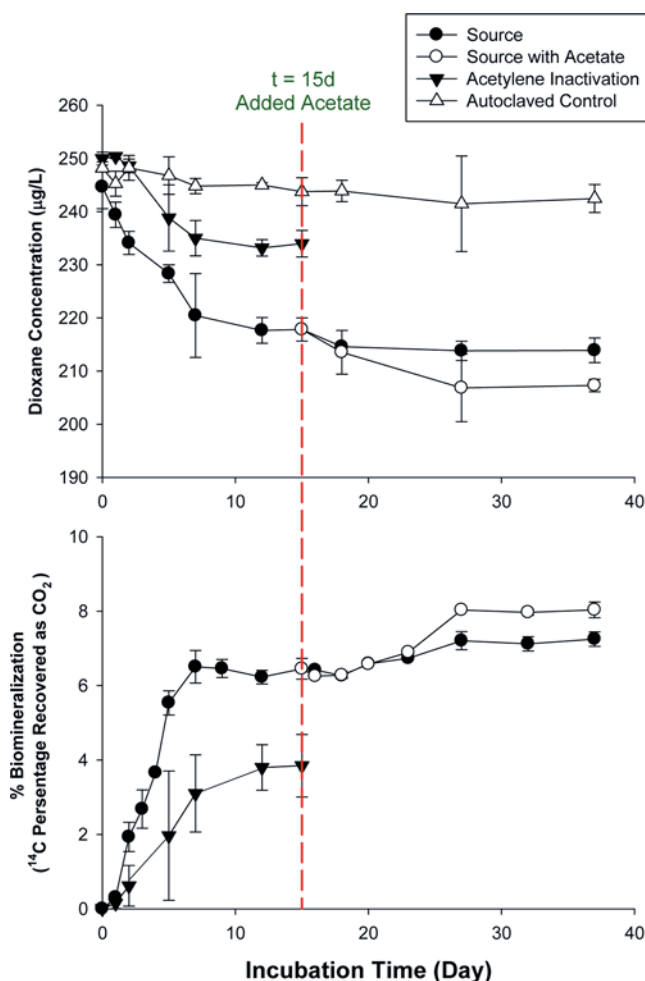
Figure 6. Dioxane degradation and the accumulated percentage of ^{14}C recovered as CO_2 in microcosms prepared with the groundwater samples collected at the source zone. The mineralization data were normalized with autoclaved controls.

precludes potential confounding effects exerted by oxygenase-inducing substrates. Significant enhancement of $^{14}CO_2$ production after amendment with acetate (Figure 6) was observed in all microcosms ($p < 0.05$), suggesting that dioxane degradation was hindered by an insufficiency of reducing cofactors (e.g., NADH) to sustain monooxygenase activity.

To further assess the crucial role of monooxygenases on dioxane transformation, microcosms were exposed to 8% acetylene in the headspace. As the simplest alkyne, acetylene inactivates a variety of bacterial monooxygenases.[53,54] Significant inactivation of both dioxane degradation and mineralization (Figure 6) was observed in microcosms exposed with acetylene. The acetylene-treated microcosms lost more than 40% of their dioxane degradation activity compared to those in untreated microcosms. This partial inactivation implies that acetylene was not a potent inactivator for some of the dioxane degraders, as is the case for some monooxygenases. For instance, toluene-2-monooxygenase in *Burkholderia cepacia* G4 was not sensitive to the inhibition of acetylene concentrations lower than 10% (v/v).[53] Furthermore, *Rhodococcus* sp. RR1 possesses a propane monooxygenase and is capable of degrading dioxane and BTEX without inhibition by acetylene.[12,13,55]

Overall, this work challenges the common notion that natural attenuation of dioxane plumes is unlikely to occur and offers a novel molecular forensic tool to assess *in situ* biodegradation processes. We also demonstrate the widespread distribution of SDIMO genes that are likely involved in dioxane degradation, suggesting the feasibility of MNA at this site. In addition, our findings infer that the diversity and spatial distribution of enzymes involved in dioxane degradation are generally underestimated, which underscores the need to develop appropriate forensic tools to rapidly quantify the presence and expression of relevant catabolic capacities.

■ ASSOCIATED CONTENT

Ⓢ Supporting Information

Experimental procedures and results, Figures S1−S5, Tables S1−S10, and references. This material is available free of charge via the Internet at http://pubs.acs.org.

■ AUTHOR INFORMATION

Corresponding Author
*E-mail: alvarez@rice.edu.

Notes
The authors declare no competing financial interest.

■ ACKNOWLEDGMENTS

■ REFERENCES

(1) Mohr, T.; Stickney, J.; DiGuiseppi, W. *Environmental Investigation and Remediation: 1,4-Dioxane and other Solvent Stabilizers*; CRC Press: 2010; p 552.

(2) IARC *Monograph on 1,4-Dioxane*; International Agency for Research on Cancer: Lyon, France, 1999.

(3) EPA http://www.epa.gov/ncea/iris/subst/0326.htm#woe (accessed Aug 12, 2013).

(4) Zenker, M. J.; Borden, R. C.; Barlaz, M. A. Occurrence and treatment of 1,4-dioxane in aqueous environments. *Environ. Eng. Sci.* **2003**, *20* (5), 423−432.

(5) Alvarez, P. J. J.; Illman, W. *Bioremediation and Natural Attenuation of Groundwater Contaminants: Process Fundamentals and Mathematical Models*; John Wiley & Sons, Inc.: 2006; p 608.

(6) Li, M.; Fiorenza, S.; Chatham, J. R.; Mahendra, S.; Alvarez, P. J. 1,4-Dioxane biodegradation at low temperatures in Arctic groundwater samples. *Water Res.* **2010**, *44* (9), 2894−900.

(7) Kim, Y. H.; Engesser, K. H.; Kim, S. J. Physiological, numerical and molecular characterization of alkyl ether-utilizing rhodococci. *Environ. Microbiol.* **2007**, *9* (6), 1497−1510.

(8) Steffan, R. J. *ER-1422: Biodegradation of 1,4-Dioxane*; Shaw Environmental, Inc.: 2007.

(9) Leahy, J. G.; Batchelor, P. J.; Morcomb, S. M. Evolution of the soluble diiron monooxygenases. *FEMS Microbiol. Rev.* **2003**, *27* (4), 449−479.

(10) Notomista, E.; Lahm, A.; Di Donato, A.; Tramontano, A. Evolution of bacterial and archaeal multicomponent monooxygenases. *J. Mol. Evol.* **2003**, *56* (4), 435−45.

(11) Thiemer, B.; Andreesen, J. R.; Schrader, T. Cloning and characterization of a gene cluster involved in tetrahydrofuran degradation in *Pseudonocardia* sp strain K1. *Arch. Microbiol.* **2003**, *179* (4), 266−277.

(12) Mahendra, S.; Alvarez-Cohen, L. Kinetics of 1,4-dioxane biodegradation by monooxygenase-expressing bacteria. *Environ. Sci. Technol.* **2006**, *40* (17), 5435−5442.

(13) Vainberg, S.; McClay, K.; Masuda, H.; Root, D.; Condee, C.; Zylstra, G. J.; Steffan, R. J. Biodegradation of ether pollutants by *Pseudonocardia* sp. strain ENV478. *Appl. Environ. Microbiol.* **2006**, *72* (8), 5218−24.

(14) Sales, C. M.; Mahendra, S.; Grostern, A.; Parales, R. E.; Goodwin, L. A.; Woyke, T.; Nolan, M.; Lapidus, A.; Chertkov, O.; Ovchinnikova, G.; Sczyrba, A.; Alvarez-Cohen, L. Genome Sequence of the 1,4-Dioxane-Degrading *Pseudonocardia dioxanivorans* Strain CB1190. *J. Bacteriol.* **2011**, *193* (17), 4549−4550.

(15) Parales, R. E.; Adamus, J. E.; White, N.; May, H. D. Degradation of 1,4-dioxane by an Actinomycete in pure culture. *Appl. Environ. Microbiol.* **1994**, *60* (12), 4527−4530.

(16) Yao, Y. L.; Lv, Z. M.; Min, H.; Lv, Z. H.; Jiao, H. P. Isolation, identification and characterization of a novel *Rhodococcus* sp strain in biodegradation of tetrahydrofuran and its medium optimization using sequential statistics-based experimental designs. *Bioresour. Technol.* **2009**, *100* (11), 2762−2769.

(17) Grostern, A.; Sales, C. M.; Zhuang, W. Q.; Erbilgin, O.; Alvarez-Cohen, L. Glyoxylate metabolism is a key feature of the metabolic degradation of 1,4-dioxane by *Pseudonocardia dioxanivorans* strain CB1190. *Appl. Environ. Microbiol.* **2012**, *78* (9), 3298−3308.

(18) Sharp, J. O.; Sales, C. M.; Alvarez-Cohen, L. Functional characterization of propane-enhanced *N*-nitrosodimethylamine degradation by two actinomycetales. *Biotechnol. Bioeng.* **2010**, *107* (6), 924−32.

(19) Fam, S. A.; Fogel, S.; Findlay, M. Rapid degradation of 1,4-dioxane using a cultured propanotroph. In *Battelle Conference: In Situ and On-Site Bioremediation Symposium*, Baltimore, Maryland, 2005.

(20) Hazen, T. C.; Dubinsky, E. A.; DeSantis, T. Z.; Andersen, G. L.; Piceno, Y. M.; Singh, N.; Jansson, J. K.; Probst, A.; Borglin, S. E.; Fortney, J. L.; Stringfellow, W. T.; Bill, M.; Conrad, M. E.; Tom, L. M.; Chavarria, K. L.; Alusi, T. R.; Lamendella, R.; Joyner, D. C.; Spier, C.; Baelum, J.; Auer, M.; Zemla, M. L.; Chakraborty, R.; Sonnenthal, E. L.; D'haeseleer, P.; Holman, H. Y. N.; Osman, S.; Lu, Z. M.; Van Nostrand, J. D.; Deng, Y.; Zhou, J. Z.; Mason, O. U. Deep-sea oil plume enriches indigenous oil-degrading bacteria. *Science* **2010**, *330* (6001), 204−208.

(21) He, Z. L.; Deng, Y.; Van Nostrand, J. D.; Tu, Q. C.; Xu, M. Y.; Hemme, C. L.; Li, X. Y.; Wu, L. Y.; Gentry, T. J.; Yin, Y. F.; Liebich, J.; Hazen, T. C.; Zhou, J. Z. GeoChip 3.0 as a high-throughput tool for analyzing microbial community composition, structure and functional activity. *ISME J.* **2010**, *4* (9), 1167−1179.

(22) Liang, Y.; Van Nostrand, J. D.; Deng, Y.; He, Z.; Wu, L.; Zhang, X.; Li, G.; Zhou, J. Functional gene diversity of soil microbial communities from five oil-contaminated fields in China. *ISME J.* **2011**, *5* (3), 403−413.

(23) Lu, Z. M.; Deng, Y.; Van Nostrand, J. D.; He, Z. L.; Voordeckers, J.; Zhou, A. F.; Lee, Y. J.; Mason, O. U.; Dubinsky, E. A.; Chavarria, K. L.; Tom, L. M.; Fortney, J. L.; Lamendella, R.; Jansson, J. K.; D'haeseleer, P.; Hazen, T. C.; Zhou, J. Z. Microbial gene functions enriched in the Deepwater Horizon deep-sea oil plume. *ISME J.* **2012**, *6* (2), 451−460.

(24) Li, M.; Conlon, P.; Fiorenza, S.; Vitale, R. J.; Alvarez, P. J. J. Rapid analysis of 1,4-dioxane in groundwater by frozen micro-extraction with gas chromatography/mass spectrometry. *Ground Water Monit. Rem.* **2011**, *31* (4), 70−76.

(25) Zhou, J. Z.; Bruns, M. A.; Tiedje, J. M. DNA recovery from soils of diverse composition. *Appl. Environ. Microbiol.* **1996**, *62* (2), 316−322.

(26) He, Z. L.; Gentry, T. J.; Schadt, C. W.; Wu, L. Y.; Liebich, J.; Chong, S. C.; Huang, Z. J.; Wu, W. M.; Gu, B. H.; Jardine, P.; Criddle, C.; Zhou, J. GeoChip: a comprehensive microarray for investigating biogeochemical, ecological and environmental processes. *ISME J.* **2007**, *1* (1), 67−77.

(27) He, Z. L.; Van Nostrand, J. D.; Deng, Y.; Zhou, J. Z. Development and applications of functional gene microarrays in the

analysis of the functional diversity, composition, and structure of microbial communities. *Front. Environ. Sci. Eng. China* **2011**, 5 (1), 1−20.

(28) He, Z.; Deng, Y.; Zhou, J. Development of functional gene microarrays for microbial community analysis. *Curr. Opin. Biotechno.l* **2012**, 23 (1), 49−55.

(29) Eisen, M. B.; Spellman, P. T.; Brown, P. O.; Botstein, D. Cluster analysis and display of genome-wide expression patterns. *Proc. Natl. Acad. Sci. U.S.A.* **1998**, 95 (25), 14863−14868.

(30) Lu, Z. M.; He, Z. L.; Parisi, V. A.; Kang, S.; Deng, Y.; Van Nostrand, J. D.; Masoner, J. R.; Cozzarelli, I. M.; Suflita, J. M.; Zhou, J. Z. GeoChip-based analysis of microbial functional gene diversity in a landfill leachate-contaminated aquifer. *Environ. Sci. Technol.* **2012**, 46 (11), 5824−5833.

(31) Garten, C. T.; Kang, S.; Brice, D. J.; Schadt, C. W.; Zhou, J. Variability in soil properties at different spatial scales (1 m-1 km) in a deciduous forest ecosystem. *Soil Biol. Biochem.* **2007**, 39 (10), 2621−2627.

(32) Zhou, J. Z.; Kang, S.; Schadt, C. W.; Garten, C. T. Spatial scaling of functional gene diversity across various microbial taxa. *Proc. Natl. Acad. Sci. U.S.A.* **2008**, 105 (22), 7768−7773.

(33) Coleman, N. V.; Bui, N. B.; Holmes, A. J. Soluble di-iron monooxygenase gene diversity in soils, sediments and ethene enrichments. *Environ. Microbiol.* **2006**, 8 (7), 1228−1239.

(34) Holmes, A. J.; Coleman, N. V. Evolutionary ecology and multidisciplinary approaches to prospecting for monooxygenases as biocatalysts. *Antonie Van Leeuwenhoek* **2008**, 94 (1), 75−84.

(35) Da Silva, M. L.; Alvarez, P. J. Assessment of anaerobic benzene degradation potential using 16S rRNA gene-targeted real-time PCR. *Environ. Microbiol.* **2007**, 9 (1), 72−80.

(36) Larkin, M. A.; Blackshields, G.; Brown, N. P.; Chenna, R.; McGettigan, P. A.; McWilliam, H.; Valentin, F.; Wallace, I. M.; Wilm, A.; Lopez, R.; Thompson, J. D.; Gibson, T. J.; Higgins, D. G. Clustal W and clustal X version 2.0. *Bioinformatics* **2007**, 23 (21), 2947−2948.

(37) Tamura, K.; Peterson, D.; Peterson, N.; Stecher, G.; Nei, M.; Kumar, S. MEGA5: Molecular evolutionary genetics analysis using maximum likelihood, evolutionary distance, and maximum parsimony methods. *Mol. Biol. Evol.* **2011**, 28 (10), 2731−2739.

(38) Oh, B. T.; Just, C. L.; Alvarez, P. J. J. Hexahydro-1,3,5-trinitro-1,3,5-triazine mineralization by zerovalent iron and mixed anaerobic cultures. *Environ. Sci. Technol.* **2001**, 35 (21), 4341−4346.

(39) Kotani, T.; Kawashima, Y.; Yurimoto, H.; Kato, N.; Sakai, Y. Gene structure and regulation of alkane monooxygenases in propane-utilizing *Mycobacterium* sp TY-6 and *Pseudonocardia* sp TY-7. *J. Biosci. Bioeng.* **2006**, 102 (3), 184−192.

(40) Connon, S. A.; Tovanabootr, A.; Dolan, M.; Vergin, K.; Giovannoni, S. J.; Semprini, L. Bacterial community composition determined by culture-independent and -dependent methods during propane-stimulated bioremediation in trichloroethene-contaminated groundwater. *Environ. Microbiol.* **2005**, 7 (2), 165−178.

(41) Murrell, J. C.; McDonald, I. R.; Gilbert, B. Regulation of expression of methane monooxygenases by copper ions. *Trends Microbiol.* **2000**, 8 (5), 221−225.

(42) Findlay, M.; Smoler, D.; Fogel, S. Dioxane-degrading propanotrophs for *in-situ* remediation. In *Battelle Conference: In Situ and On-Site Bioremediation Symposium*, Baltimore, Maryland, 2007.

(43) Yuen, T.; Wurmbach, E.; Pfeffer, R. L.; Ebersole, B. J.; Sealfon, S. C. Accuracy and calibration of commercial oligonucleotide and custom cDNA microarrays. *Nucleic Acids Res.* **2002**, 30, (10).

(44) Alvarez, P. J. J.; Cronkhite, L. A.; Hunt, C. S. Use of benzoate to establish reactive buffer zones for enhanced attenuation of BTX migration: Aquifer column experiments. *Environ. Sci. Technol.* **1998**, 32 (4), 509−515.

(45) Capiro, N. L.; Da Silva, M. L. B.; Stafford, B. P.; Rixey, W. G.; Alvarez, P. J. J. Microbial community response to a release of neat ethanol onto residual hydrocarbons in a pilot-scale aquifer tank. *Environ. Microbiol.* **2008**, 10 (9), 2236−2244.

(46) Smith, C. A.; Hyman, M. R. Oxidation of gasoline oxygenates by closely related non-haem-iron alkane hydroxylases in *Pseudomonas mendocina* KR1 and other n-octane-utilizing *Pseudomonas* strains. *Environ. Microbiol. Rep.* **2010**, 2 (3), 426−432.

(47) McKelvie, J. R.; Hyman, M. R.; Elsner, M.; Smith, C.; Aslett, D. M.; Lacrampe-Couloume, G.; Lollar, B. S. Isotopic fractionation of methyl tert-butyl ether suggests different initial reaction mechanisms during aerobic biodegradation. *Environ. Sci. Technol.* **2009**, 43 (8), 2793−2799.

(48) Collett, T. S. Natural-gas hydrates of the Prudhoe Bay and Kuparuk River Area, North Slope, Alaska. *AAPG Bull.* **1993**, 77 (5), 793−812.

(49) Fields, M. W.; Yan, T. F.; Rhee, S. K.; Carroll, S. L.; Jardine, P. M.; Watson, D. B.; Criddle, C. S.; Zhou, J. Z. Impacts on microbial communities and cultivable isolates from groundwater contaminated with high levels of nitric acid-uranium waste. *FEMS Microbiol. Ecol.* **2005**, 53 (3), 417−428.

(50) Waldron, P. J.; Wu, L. Y.; Van Nostrand, J. D.; Schadt, C. W.; He, Z. L.; Watson, D. B.; Jardine, P. M.; Palumbo, A. V.; Hazen, T. C.; Zhou, J. Z. Functional gene array-based analysis of microbial community structure in groundwaters with a gradient of contaminant levels. *Environ. Sci. Technol.* **2009**, 43 (10), 3529−3534.

(51) Mahendra, S.; Petzold, C. J.; Baidoo, E. E.; Keasling, J. D.; Alvarez-Cohen, L. Identification of the intermediates of in vivo oxidation of 1, 4-dioxane by monooxygenase-containing bacteria. *Environ. Sci. Technol.* **2007**, 41 (21), 7330−6.

(52) Criddle, C. S. The Kinetics of Cometabolism. *Biotechnol. Bioeng.* **1993**, 41 (11), 1048−1056.

(53) Yeager, C. M.; Bottomley, P. J.; Arp, D. J.; Hyman, M. R. Inactivation of toluene 2-monooxygenase in *Burkholderia cepacia* G4 by alkynes. *Appl. Environ. Microbiol.* **1999**, 65 (2), 632−639.

(54) Prior, S. D.; Dalton, H. Acetylene as a suicide substrate and active-site probe for methane monooxygenase from *Methylococcus-Capsulatus* (Bath). *FEMS Microbiol. Lett.* **1985**, 29 (1−2), 105−109.

(55) Burback, B. L.; Perry, J. J. Biodegradation and biotransformation of groundwater pollutant mixtures by *Mycobacterium vaccae*. *Appl. Environ. Microbiol.* **1993**, 59 (4), 1025−9.